Quantitative Mapping of Strain Defects in Multidomain Quantum Materials

Michelle Smeaton[1], Ismail El Baggari[2], Daniel Balazs[3], Tobias Hanrath[3] and Lena Kourkoutis[4]

[1]Department of Materials Science and Engineering, Cornell University, United States, [2]The Rowland Institute at Harvard University, United States, [3]Smith School of Chemical and Biomolecular Engineering, Cornell University, United States, [4]School of Applied and Engineering Physics, Cornell University, United States

Strain mapping provides important insights into defect structures which affect materials properties in a variety of ways. While phase-based methods such as geometric phase analysis (GPA) are commonly used to investigate such structures [1], these methods have the drawback of requiring a fixed reference lattice from which the strain is quantified. For material systems where strain features are of interest over fields of view containing many crystalline domains, a global reference lattice cannot be effectively used. Additionally, the accuracy of phase retrieval methods is limited when applied to high magnitude, nonuniform strain states [2]. Here we present an alternative approach based on local sine wave fitting, which allows us to extract tensile strain and lattice rotation maps over ~100 nm fields of view with near unit cell-level resolution and uncertainty on the order of 0.1% without requiring a reference lattice [3]. As a model system, we consider epitaxially connected quantum dot (QD) superlattices, where each QD represents an individual crystalline domain and which contain several types of strain defects primarily in the connections between QDs. The defects in these materials prevent electronic coupling between QDs and lead to superlattice disorder, impeding electronic transport and preventing realization of theoretically predicted tunable band structures.

In Fig. 1a, we illustrate the challenge of applying a phase-based strain mapping method to a monolayer QD superlattice. For the ADF-STEM image in panel one, we map the phase gradient with respect to vector $\mathbf{q_a}$ for reference lattice vectors, $\mathbf{q_{a1}}$ and $\mathbf{q_{a2}}$ defined by two reference QDs as outlined in green and yellow, respectively. For small distortions, this would be equivalent to tensile strain. However, because relatively large rotations between QD atomic lattices are involved, the maps cannot be interpreted in this way. This is made doubly clear by the stark differences between the maps resulting from the two references and the nonphysical, widespread distortions suggested in each map.

Our approach, which builds on a method formerly developed for scanning tunneling microscopy [4], is outlined in Fig. 1b. For the same ADF-STEM image shown in Fig. 1a, we Fourier filter a pair of Bragg peaks for each lattice direction (e.g., $\mathbf{a}$ and $\mathbf{b}$ in Fig. 1a) independently, ensuring that all intensity from those peaks is captured. This results in a real-space image containing only information from the frequencies of interest as shown in the first panel of Fig. 1b for the frequencies encompassed by the dotted circle in the Fourier transform in Fig. 1a. We subsequently fit 2D sine functions to subsets of this image, defined by a grid of small, overlapping windows. The functional form, along with an example of a fit window and the resulting fit are shown in Fig. 1b, panel two. Finally, we calculate the tensile strain and lattice rotation from the extracted lattice spacing, λ, and rotation, θ, respectively (Fig. 2). The resulting tensile strain map for the $\mathbf{a}$ lattice direction is shown in the third panel of Fig. 1b. Here, as expected, the majority of the field of view exhibits approximately zero tensile strain, while some QD connections show high intensity features, clearly indicating tensile defects.

Using this method, we can differentiate between four distinct strain defect types in QD connections (Fig 2). Tensile strain maps indicate tensile defects as well as edge dislocations, while rotation maps highlight shear and bending defects. For each defect type, Fig. 2 shows the initial ADF-STEM image with the

defect present in the QD connection, a schematic representation of the defect in the relevant lattice fringes, and the tensile strain or rotation map for those same fringes. Tensile and shear defects are identified by high intensity features in the tensile strain and rotation maps, respectively, edge dislocations are identified by a dumbbell feature around the dislocation core, and bending defects are identified by changes in rotation value between neighboring QDs. Furthermore, tracking these strain defects over large fields of view with this method couples well with *in situ* STEM, revealing not only the various types of defects but also how each evolves with heating [3].
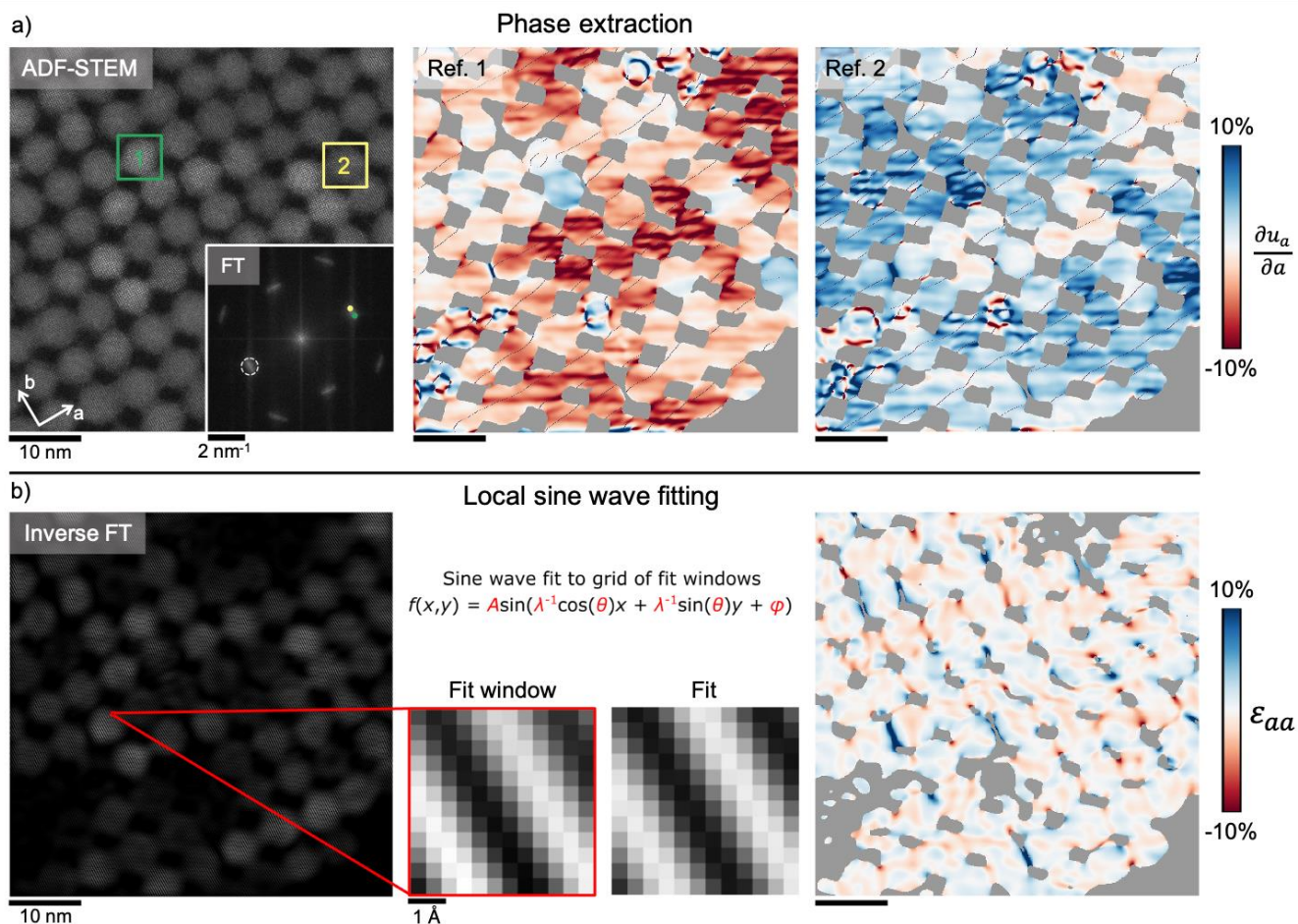
Figure 1. (a) Application of phase-based strain mapping to a monolayer QD superlattice for two reference frames. From left to right: a raw ADF-STEM image with inset Fourier transform (FT) and the gradient of the phase with respect to reference lattice vector qa, mapped for the same field of view for reference lattices 1 and 2. The QDs used to define references 1 and 2 are outlined in the ADF image, and the resulting lattice vectors of interest, qa1 and qa2, are marked in the FT in green and yellow, respectively. (b) Local sine wave fitting method overview. From left to right: real-space image resulting from Fourier filtering the ADF image in (a) with the mask indicated by the dotted circle in the inset FT, form of the 2D wave function used for fitting and example of a fit window and resulting fit, and resulting tensile strain map. The map shows the tensile strain is approximately zero for most QDs, with a few high strain features at QD connections denoting tensile defects.
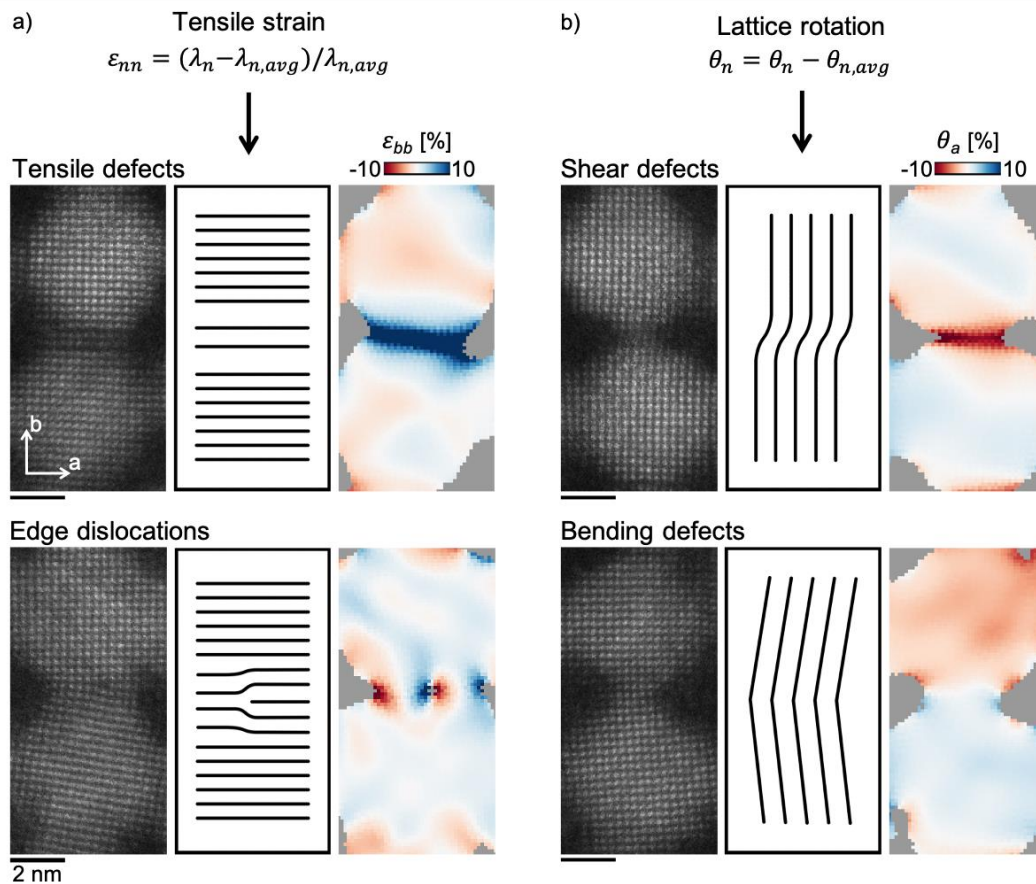
Figure 2. Examples of strain defects identified through local sine wave fitting. (a) Equation for tensile strain, εnn, calculated from lattice spacing, λn, and the average lattice spacing, λn,avg, of the QD cores, and examples of tensile and edge dislocations and their resulting tensile strain features. (b) Equation for the lattice rotation, θn, calculated as the difference from the average lattice rotation, θn,avg, and examples of shear and bending defects and their resulting lattice rotation features. For each defect example, from left to right: the raw ADF-STEM image, a schematic representation of the defect in the relevant lattice fringes, and the tensile strain or rotation map for the same fringes.

References
[1] M.J. Hytch *et al.*, Ultramicroscopy. **74** (1998), p. 131.
[2] H. Zhang *et al.*, Ultramicroscopy. **171** (2016), p. 34.
[3] M.A. Smeaton *et al.*, ACS Nano. **15** (2021), p. 719.
[4] Á. Pásztor *et al.*, Phys. Rev. Res. **1** (2019), p. 033114.
[5] This work is supported by DOE (DE-SC0018026) and NSF (DMR-1719875, DGE-1650441).